Electronic Supplementary Material (ESI) for Journal of Materials Chemistry A.

Supporting Information

Directed solution transfer of 3D solar evaporator inhibiting salt crystallization

Ye Peng,[a] Xinzhen Zhao,[ab] Changkun Liu [a] *

[a] College of Chemistry and Environmental Engineering, Shenzhen University,

Shenzhen 518060, P.R. China

[b] Midea Corporate Research Center, Foshan, 528311, P.R. China

∗E-mail: liuck@szu.edu.cn

Section S1. Estimation of evaporation performance

The evaporation rate (υ, kg m^{-2} h^{-1}) and solar evaporation efficiency (η, %) were calculated according to the following formulas (Se. 1) and (Se. 2):

$$\upsilon = \frac{\Delta m}{St} \quad \text{(Se. 1)}$$

$$\eta = \frac{(\upsilon - \upsilon_d)H_t}{P_{solar}} \times 100\% \quad \text{(Se. 2)}$$

where Δm (kg) is the weight loss value, and t (h) is the time of solar evaporation. The top area (7.065 cm^2) of the evaporator is used as the effective evaporation area S (m^2). P_{solar} (1000 W m^{-2}) is the irradiation intensity of the Xenon lamp. υ_d (kg m^{-2} h^{-1}) is the evaporation rate under dark condition. H_t is evaporation enthalpy of the pure water.

The (Se. 3), (Se. 4) and (Se. 5) were used to calculate the enthalpy of evaporation of pure water (H_t).

$$H_t = h_{lv} + C\Delta T \quad \text{(Se. 3)}$$

$$h_{lv} = \alpha + \beta T_1 + \gamma T_1^{1.5} + \delta T_1^{2.5} + \varepsilon T_1^{3} \quad \text{(Se. 4)}$$

$$H_{eq} m_0 = H_t m_g \quad \text{(Se. 5)}$$

where h_{lv} is latent heat of phase change, C is specific heat capacity of water (4.2 kJ kg^{-1} K^{-1}), ΔT is the temperature increment of the bulk water, and T_1 is the equilibrium temperature (°C) of the top evaporation interface. α = 2500.304, β = -2.2521025, γ = -0.021465847, δ = 3.1750136×10^{-4}, and ε = -2.8607959×10^{-5}, which are all constants.

It is worth noting that the evaporation enthalpy of the ER-4 is reduced due to the increase of the proportion of the intermediate water in the presence of hydrogels. Therefore, a special experiment was introduced in order to recalculate the enthalpy of evaporation. The water and

ER-4 with the same evaporation area were set in a closed container with supersaturated magnesium chloride solution (Fig. S1a).[S1] The mass changes of them after 10 h were measured, and the real evaporation enthalpy change (Fig.S1b) was obtained by (Se. 5), where m_0 and m_g are the mass changes of the water and ER-4 in the dark (Fig. S1c).

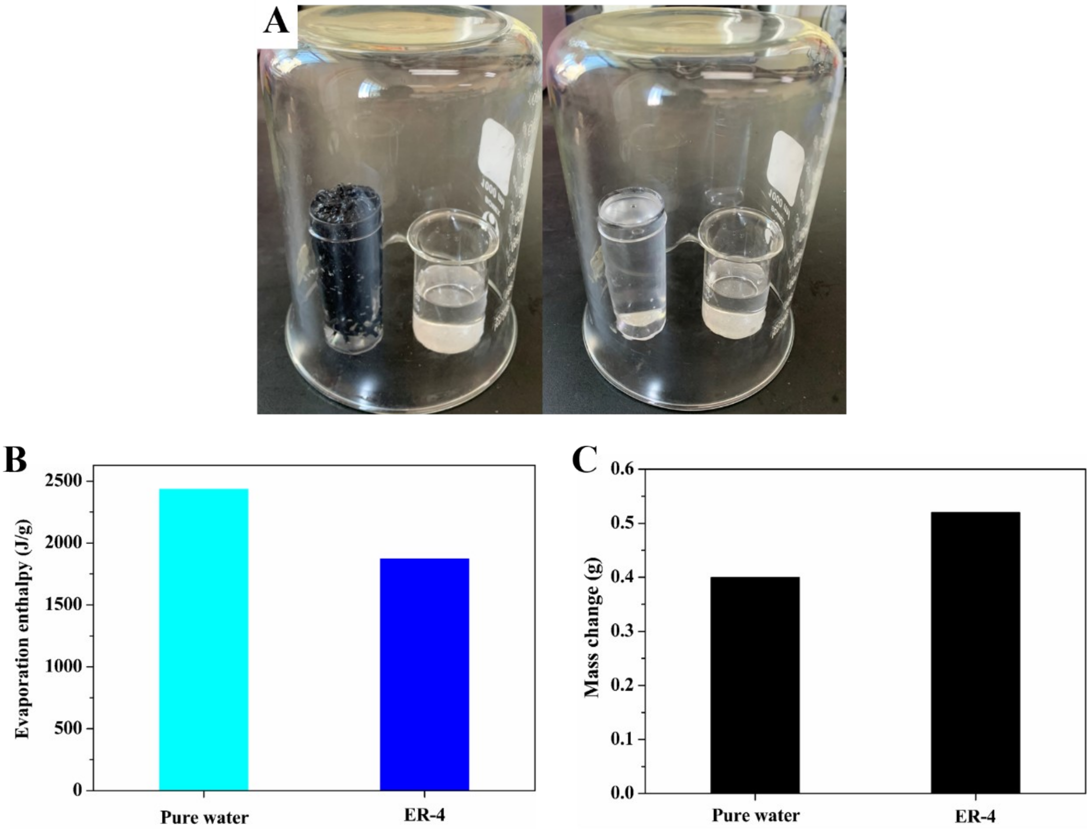

Fig. S1. The quality changes of ER-4 and pure water were tested (with supersaturated magnesium chloride solution) under dark closed conditions (A), the evaporation enthalpy of pure water and ER-4 (B) and the mass changes of pure water and ER-4 after 10 h (C).

Section S2. Sample information

Table S1 Information of ER-4

Number of rGO-PSC-4	Top diameter	*Top area	Side length	*Side area	Root length
40	3cm	7.065cm^2	3cm	28.26 cm^2	6cm

* The radius of the top (r) and side length (l) were measured with a ruler, and the top area and side area of the evaporator were calculated with the following area formulas: $S_{top} = \pi r^2$, $S_{side} = 2\pi rl$.

Section S3. Comparison of the cost and performance of solar evaporator

Table S2 Comparison of the cost of the solar evaporator

Materials	Cost ($\$/m^2$)	Evaporation rate ($kg\ m^{-2}\ h^{-1}$)	**Cost effectiveness ($g\ h^{-1}\ \$^{-1}$)	Ref.
rGO-agarose Cellulose sponge	14.38	4.35	302.5	S2
Solar vacuum tube	110.34	0.7	6	S3
Ti_2O_3/ PVA hydrogel	293.21	3.6	12.3	S4
Selective solar absorber	54	0.5	9	S5
PVA hydrogel	98.83	3.2	32.4	S6
Aluminum sheet/ Al NPs	6600	1.43	0.2	S7
Balsa wood/CNT	31.04	0.95	30.6	S8
Polypyrene/Stainless steel meshes	55	0.92	16.7	S9
ER-4	83.34	4.57	54.8	This work

** The Cost-effectiveness (ε) is defined as $\varepsilon = v/c$, where v refers to the evaporation rate ($kg\ m^{-2}\ h^{-1}$) and c is the materials cost ($\$\ m^{-2}$). The ε can be interpreted as the amount of the purified water produced in 1 h per 1 dollar spent.

Table S3 Comparison of the performance of the solar evaporator

Materials	Evaporation rate kg m^{-2} h^{-1}	Evaporation efficiency %	Ref.	Year
C-corncob	4.16	~130%	S10	2021
PU/CNT2/ZCB	~2.2	93.5	S11	2021
3D HCE	7.6	178.6	S12	2021
Carbon bread sponge	1.28	85	S13	2021
3D porous carbon foam	1.37	93.7	S14	2021
PSSE-N55-H6	3.72	-	S15	2021
Cuo/Cu-CB	1.65	96.7	S16	2020
3D T-shaped porous sponge	1.47	89.1	S17	2020
Biomass-Derived Hybrid Hydrogel Evaporators	3.2	90	S18	2020
Tailoring Nanoscale Surface Topography of Hydrogel	2.6	91	S19	2019
Graphene based hive	1.95	85	S20	2019
Graphene/C aerogel	1.56	90	S21	2019
ER-4	4.57	122	This work	2021

Section S4. Energy analysis and thermal conductivity of solar evaporation system

Because ER-4 had the characteristics of reducing heat loss and recovering environmental energy, it could achieve high evaporation rate and evaporation efficiency. In order to further explain this, the following formula is used to analyze the energy exchange of ER-4:

$$E_{environment} = -A_1\varepsilon\sigma\left(T_1^4 - T_0^4\right) - A_2\varepsilon\sigma\left(T_2^4 - T_0^4\right) - A_1h\left(T_1 - T_0\right) - A_2h\left(T_2 - T_0\right) - C\Delta T \quad \text{(Se. 6)}$$

where A_1 is the area of the top surface of ER-4 (7.065cm^2), T_1 is the average surface temperature of the top surface (~ 26.35 °C), A_2 is the side surface area (28.26 cm^2), T_2 is the average surface temperature of the side wall (~ 15.4 °C), T_0 is the ambient temperature (22 °C), ε is emissivity of the absorbing surface (~0.90), σ is the Stefan–Boltzmann constant (5.67×10^{-8} Wm^{-2} K^{-4}), h is the convection heat transfer coefficient (assumed to be 5 W m^{-2} K^{-1}), and $C\Delta T$ is the energy exchange between the bulk water and the solar evaporation system, which is 0 W due to the little change of the temperature of the bulk water. According to the above formula, the radiation loss and the convection loss from the top evaporation surface are estimated to be 0.0164 W and 0.0154 W respectively, while the radiation energy gain and the convection energy gain of the side evaporation surface from environment are estimated to be 0.0946 W and 0.0932 W. Therefore, ER-4 gets the net energy gain of 0.156 W (the energy of the incident light is 0.7056 W).

Table S4 Thermal conductivity test conditions for rGO-PSC

Hot part temperature (℃)	Cold part temperature (℃)	***Thickness (mm)	Heat quantity (W)	Pressure (Psi)	Thermal resistance (K cm^2 W^{-1})
67.27	32.37	0598	14.41	20.02	15.447

*** Due to the experimental requirements, the cotton rope for preparing rGO-PSC was replaced with cotton flakes.

Table S5 Thermal conductivity (W m^{-1} K^{-1}) of the solar evaporation system

rGO-PSC	Cotton	Insulation and drip collection lay		Container	Bulk water
		（Polystyrene foam）	(PP)	(PP)	
0.387	0.02	0.08	0.3	0.3	~0.5

Section S5. The treatment effect of the actual seawater

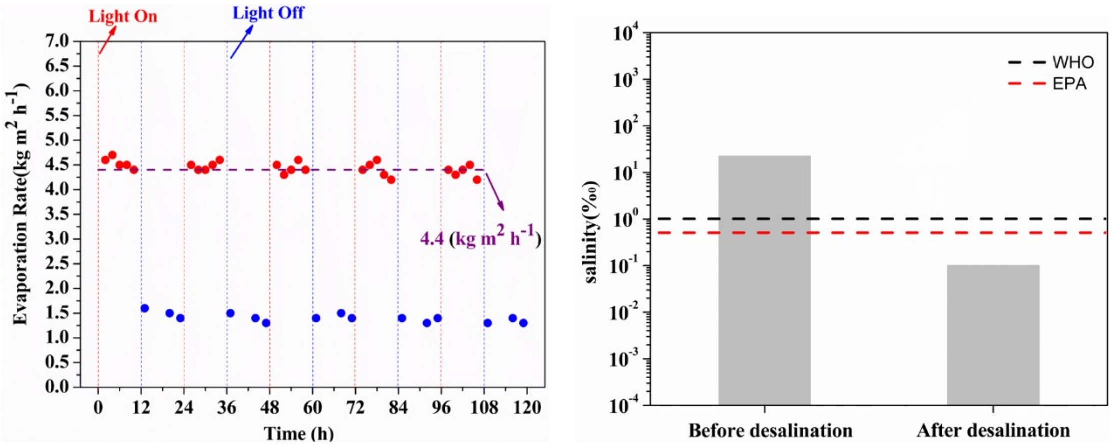

Fig. S2. Long-term evaporation rate of ER-4 in real seawater (from Bohai) and salinity of real seawater (22.4 ‰) and collected water (0.1 ‰)

Section S6. Verification of salt ion transfer and salt ablation experiment

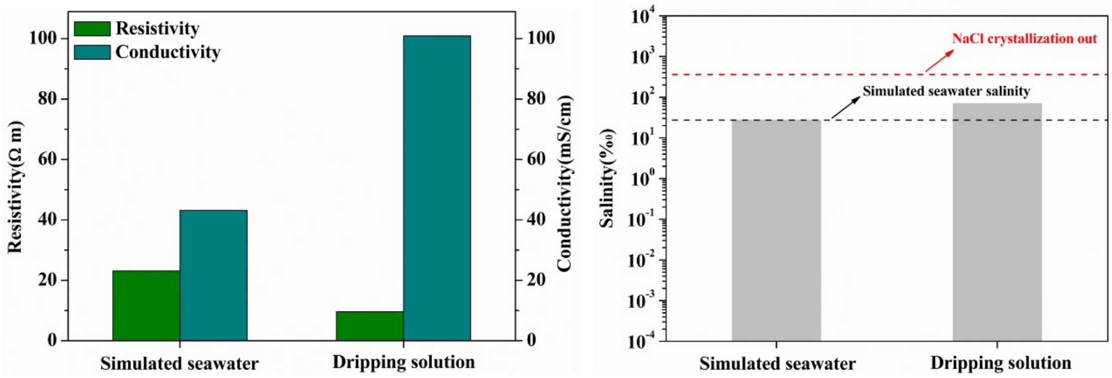

Fig. S3. The resistivity, conductivity and salinity of the simulated seawater and the dripping solution.

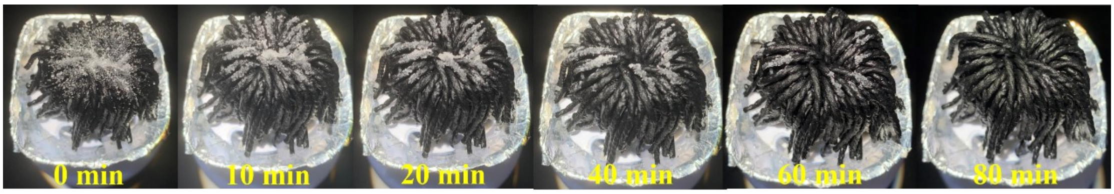

Fig. S4. The salt ablation experiment on the surface of the ER-4.

Reference:

S1. X. Y. Zhou, F. Zhao, Y. H. Guo, Y. Zhang and G. H. Yu, Energ. Environ. Sci., 2018, 11, 1985-1992.

S2. Y. D. Wang, T. Wu, Y. Lu, X. F. Yang, G. Y. Chen, G. Owens and H. L. Xu, *Nano Energy*, 2021, **78**, 105477.

S3. C. Chang, P. Tao, J. L. Xu, B. W. Fu, C. Y. Song, J. B. Wu, W. Shang and T. Deng, *ACS Appl. Mater. Interfaces,* 2019, **11**, 18466-18474.

S4. Guo, Y., Zhou, X., Zhao, F., Bae, J., Rosenberger, B., & Yu, G. (2019). *ACS Nano*, 13, 7913-7919.

S5. G. Ni, G. Li, S. V. Boriskina, H. X. Li, W. L. Yang, T. J. Zhang and G. Chen, *Nat. Energy*, 2016, **1**, 16126.

S6. F. Zhao, X. Y. Zhou, Y. Shi, X. Qian, M. Alexander, X. P. Zhao, S. Mendez, R. G. Yang, L. T. Qu and G. H. Yu, *Nat. Nanotechnol.,* 2018, **13**, 489-495.

S7. L. Zhou, Y. L. Tan, J. Y. Wang, W. C. Xu, Y. Yuan, W. S. Cai, S. N. Zhu and J. Zhu, *Nat. Photonics*, 2016, **10**, 393-398.

S8. W. Wang, J. Giltinan, S. Zakharchenko and M. Sitti, *Sci. Adv.,* 2017, **3**, e1602522.

S9. L. Zhang, B. Tang, J. Wu, R. Li and P. Wang, *Adv. Mater.,* 2015, **27**, 4889.

S10. Y. Sun, Z. B. Zhao, G. Y. Zhao, L. X. Wang, D. Z. Jia, Y. Z. Yang, X. G. Liu, X. Z. Wang and J. S. Qiu, *Carbon,* 2021, **179**, 337-347.

S11. C. Y. Wen, H. S. Guo, J. Yang, Q. S. Li, X. Y. Zhang, X. J. Sui, M. Y. Cao and L. Zhang, *Chem. Eng. J.,* **2021**, 421, 130344

S12. T. Gao, X. Wu, Y. D. Wang, G. Owens and H. L. Xu, *Sol. RRL,* 2021, **5**, 2100053.

S13. Y. Yang, M. Zhao, Z. Cao, Z. Ge, Y. F. Ma and Y. S. Chen, *RSC Adv.,* 2021, **11**, 8674.

S14. X. H. Liu, D. D. Mishra, Y. K. Li, L. Gao, H. Y. Peng, L. Zhang and C. Q. Hu, *ACS Sustain. Chem. Eng.,* 2021, **9**, 4571-4582.

S15. Z. J. Xie, Z. T. Zhu and L. B. Zhang, *ACS Appl. Mater. Interfaces,* 2021, **13**, 9027-9035.

S16. Y. Guo, Y. J. Sui, J. J. Zhang, Z. S. Cai and B. Xu, *J. Mater. Chem. A,* 2020, **8**, 25178.

S17. Q. C. Huang, X. C. Liang, Zhang, J. X, C, Y. Yan, J. Liang, T. Hao and Y. Z. Liu, *Desalination,* 2020, **499**, 114806.

S18. Y. H. Guo, H, Y. Lu, F. Zhao, X, Y. Zhou, W. Shi and G. H. Yu, *Adv. Mater.,* 2019, **32**, 1907061.

S19. Y. H. Gao, F. Zhao, X, Y. Zhou, Z, C. Chen and G. H. Yu, *Nano Lett.,* 2019, **19**, 2530-2536.

S20. X. Song, H. Song, S. Wang, J. Liu, L. Zhou, J. Xu and K. Chen, *J. Mater. Chem. A,* 2019,**7**, 26496-26503.

S21. B. Huo, D. Jiang, X. Cao, H. Liang, Z. Liu, C. Li and J. Liu, *Carbon*, 2019, **142**, 13-19.